JOURNAL OF SPACECRAFT AND ROCKETS
Vol. 30, No. 5, September–October 1993

Aerodynamic Characteristics of the HL-20

George M. Ware* and Christopher I. Cruz†
NASA Langley Research Center, Hampton, Virginia 23681

Wind-tunnel tests were made from subsonic to hypersonic speeds to define the aerodynamic characteristics of the HL-20 lifting-body configuration. The data have been assembled into an aerodynamic database for flight analysis of this proposed vehicle. The wind-tunnel data indicated that the model was longitudinally and laterally stable (about a center-of-gravity location of 0.54 body length) over the test range from Mach 20 to 0.3. At hypersonic speeds, the HL-20 model trimmed at a lift/drag (*L/D*) ratio of 1.4. This value gives the vehicle a crossrange capability similar to that of the Space Shuttle. At subsonic speeds, the HL-20 has a trimmed *L/D* ratio of about 3.6. Replacing the flat-plate outboard fins with fins having an airfoil shape increased the maximum subsonic trimmed *L/D* to 4.2.

Nomenclature

THE longitudinal data are referred to the stability-axis system and the lateral-directional data to the body-axis system (Fig. 1). All coefficients are based on the dimensions of the basic body without fins. The data are normalized by the planform area, length, and span of the body. The moment reference center was located at the vehicle center of gravity that is at 54% of the body length from the nose for all models.

b = body span, ft
cg = center of gravity
C_D = drag coefficient, drag/qS_{ref}
C_L = lift coefficient, lift/qS_{ref}
C_l = rolling-moment coefficient, rolling moment/$qS_{ref}b$
$C_{l\beta}$ = rolling-moment coefficient curve slope per degree of sideslip
C_m = pitching-moment coefficient, pitching moment/$qS_{ref}l$
C_n = yawing-moment coefficient, yawing moment/$qS_{ref}b$
$C_{n\beta}$ = yawing-moment coefficient curve slope per degree of sideslip
C_Y = side-force coefficient, side-force/qS_{ref}
$C_{Y\beta}$ = side-force coefficient curve slope per degree of sideslip
l = body length, ft
M = Mach number
q = freestream dynamic pressure, lb/ft^2
R_N = Reynolds number
S_{ref} = basic body planform area (excluding tip fins), ft^2
ΔC_l = rolling-moment coefficient increment per degree of elevon, body flap, or rudder deflection
ΔC_n = yawing-moment coefficient increment per degree of elevon, body flap, or rudder deflection
ΔC_Y = side-force coefficient increment per degree of elevon, body flap, or rudder deflection
α = angle of attack, deg
β = angle of sideslip, deg
δa = aileron (differential pitch) control deflection angle (δ_e,$L-\delta_e$,R)/2 or (δ_{BF},$L-\delta_{BF}$,R) /2
δ_{BF} = body-flap deflection angle, (positive when deflected downward), deg
δ_e = elevon deflection angle, (positive when deflected downward), deg
δ_r = vertical-fin deflection angle, (positive when deflected with the trailing edge to the left), deg

Subscripts

max = maximum value
L = left
R = right
trim = trimmed condition (zero moment)

Introduction

Early tests at the Langley Research Center indicated that the HL-20 lifting-body configuration had characteristics that made it attractive for use as a manned spacecraft.[1] Because of its favorable aerodynamic characteristics and other considerations, the HL-20 was selected for study as the orbiter configuration for the personnel launch system (PLS). Consequently, a series of wind-tunnel tests was conducted to fully define the aerodynamics of the HL-20 from hypersonic to subsonic speeds.[2–7] The data were assembled into an aerodynamic database suitable as input to batch and real-time flight simulation and analysis programs. Some of the results of these analyses, which include vehicle entry trajectory,[8] landing/subsonic handling,[9] and abort,[10] are given in the other articles in

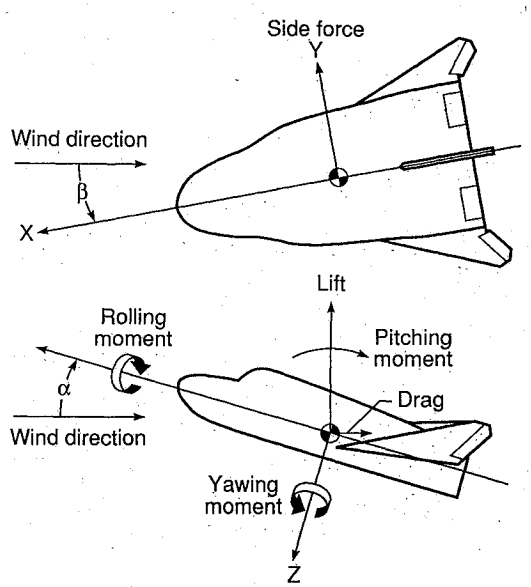

Fig. 1 Sketch of axes system used in investigation.

Presented as Paper 91-3215 at the AIAA 9th Applied Aerodynamics Conference, Baltimore, MD, September 23–25, 1991; received Dec. 3, 1992; revision received Feb. 12, 1993; accepted for publication Feb. 18, 1993.

*Senior Aerospace Engineer, Vehicle Analysis Branch, Space Systems Division. Member AIAA.

†Aerospace Engineer, Vehicle Analysis Branch, Space Systems Division. Member AIAA.

this special issue. The present article will describe the basic static aerodynamic characteristics of the HL-20 as determined from wind-tunnel tests.

Wind-Tunnel Models and Facilities

There were three different sized models tested: a 5-ft, a 20-in., and several 6-in. long models. Sketches of the 20-in. model are presented in Fig. 2. The HL-20 configuration consists of a low-aspect-ratio body with a flat undersurface and blunt base. The upper aft body was upswept at about 10 deg to give the model a built-in negative body-flap deflection. Three fins are mounted on the upper aft portion of the model. The centerline fin is relatively small, and the larger outboard fins are set at a dihedral angle of 50 deg, a toe-in angle of 1.2 deg, and an incidence angle at the body intersection of 6.6 deg. The baseline fins have a thick flat-plate cross section with a cylindrical leading edge and blunt trailing edge. Later in the investigation, the outboard fins were replaced with fins with an airfoil cross section. Control surfaces, referred to as elevons, make up the trailing edges of the outboard fins. In addition, the models have four body-flap control surfaces: two on the upper body and two on the lower body. The body flaps could only be deflected outward. For positive body-flap deflection, the lower body flaps move downward, while the upper body flaps remain undeflected. For negative body-flap deflection, the upper body flaps move upward and the lower body flaps remain undeflected. Braking action (energy management) during entry is accomplished by deflecting all four body-flap panels simultaneously.

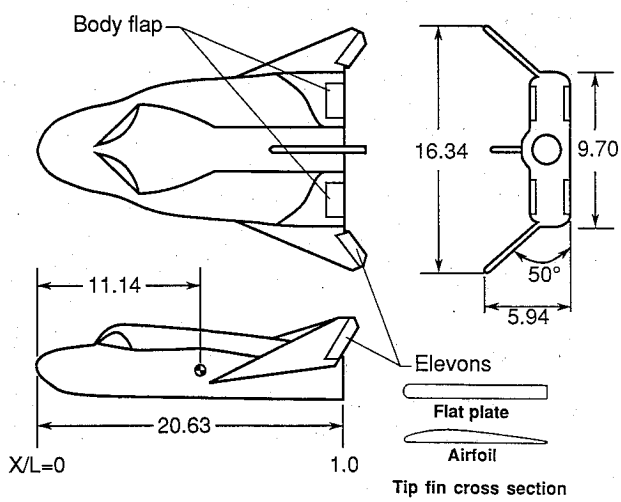

Fig. 2 Sketch of HL-20 model. All linear dimensions are in inches.

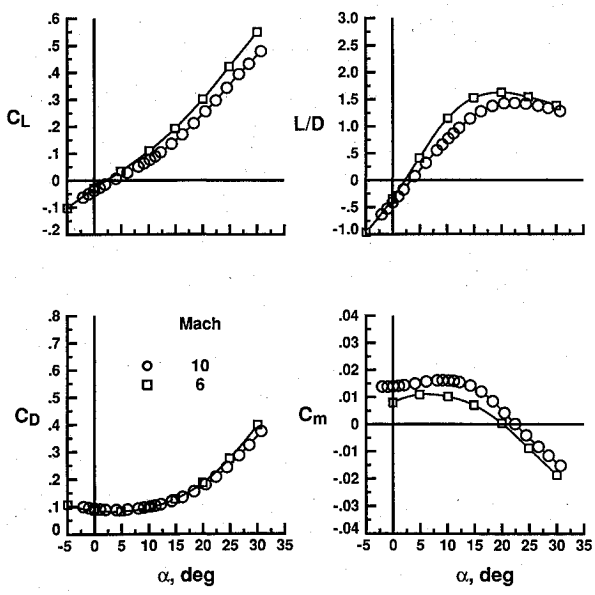

Fig. 3 Longitudinal aerodynamic characteristics at hypersonic speeds.

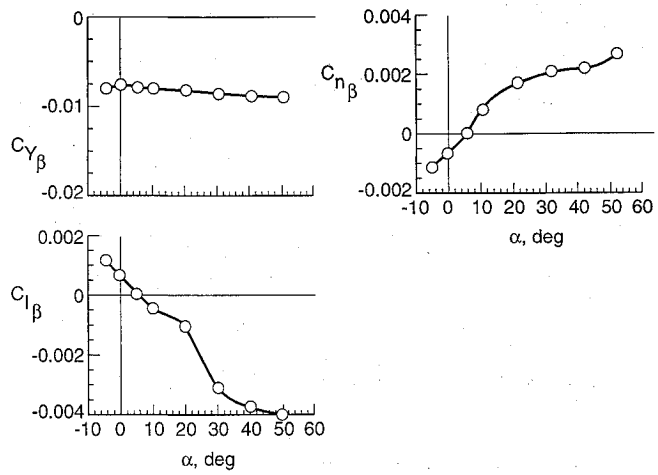

Fig. 4 Directional stability characteristics at hypersonic speeds.

Table 1 Facilities used in the investigation

Test facility	Mach number	Number of runs	Type of test
Full-Scale Tunnel	0.1	130	Force and moment
Low-Turbulence Pressure Tunnel	0.2	139	Force and moment
7×10 High-Speed Tunnel	0.3–0.8	184	Force and moment
CALSPAN 8-ft Transonic Tunnel	0.6–1.2	244	Force and moment
Unitary Plan Wind Tunnel	1.6–4.5	412	Force and moment
20-in. M=6 Hypersonic Tunnel	6	126	Force and moment thermal mapping visualization
CF_4 M=6 Hypersonic Tunnel	6	73	Force and moment thermal mapping visualization
31-in. M=10 Hypersonic Tunnel	10	83	Force and moment thermal mapping visualization
22-in. M=20 Hypersonic Tunnel	20	26	Force and moment
MSFC 14-in.Trisonic Tunnel	1.5–4.5	28	Force and moment

Tests were made in eight wind tunnels at the Langley Research Center and one each at the Calspan Corporation and Marshall Space Flight Center. The facility, Mach number range, number and types of runs in each facility are given in Table 1. A general description of these facilities is given in Ref. 11.

Aerodynamic Characteristics

Hypersonic Speeds

In Fig. 3, stable longitudinal trim (about a *cg* at 54% body length) is shown to occur at about 23- or 24-deg angle of attack at Mach 10 and 6. The lift/drag (L/D) ratio value at trim was about 1.4, which is near $(L/D)_{max}$. This L/D value gives the HL-20 a crossrange capability greater than the 1100 n.mi. of the Shuttle. (For a discussion of the crossrange characteristics of the HL-20 and impact of returning from the Space Station Freedom, see the article by Stone in this issue.[1])

The lateral data are presented as the variation of the directional stability parameter C_{n_β} and effective dihedral parameter C_{l_β}. These data were obtained by measuring the slope of the lateral coefficients with sideslip at various angles of attack. In the lateral plane,

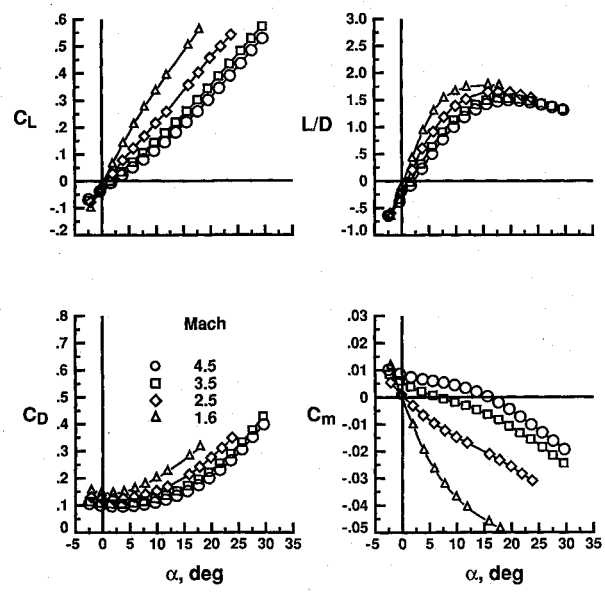

Fig. 5 Longitudinal aerodynamic characteristics at supersonic speeds.

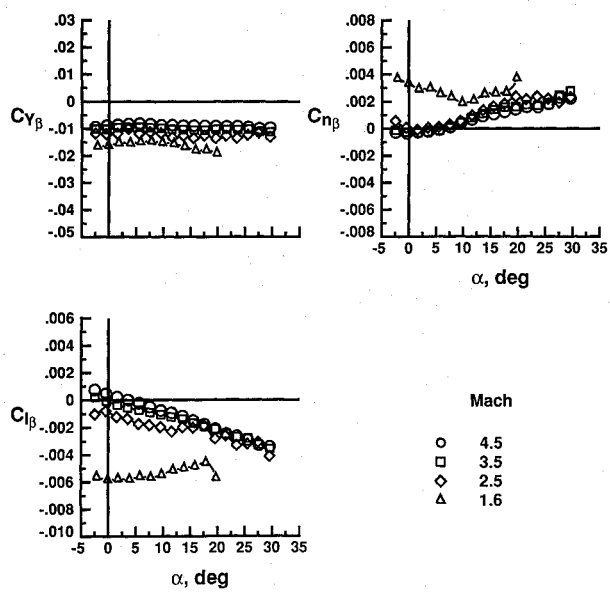

Fig. 6 Lateral aerodynamic characteristics at supersonic speeds.

Fig. 4, the model is directionally stable (positive values of C_{n_β}) with positive effective dihedral (negative values of C_{l_β}) at these hypersonic conditions above α=6 deg.

Supersonic Speeds

In the supersonic flight regime, there is no particular need in the PLS mission for the spacecraft to have high *L/D* performance because crossranging has been accomplished at higher speeds. The philosophy then is to traverse this speed range with a degree of stability and have enough control authority to navigate to the desired landing site.

The supersonic characteristics were determined from tests at Mach numbers from 4.5 to 1.6 at increments of 0.5. Sample data are presented for Mach 4.5, 3.5, 2.5, and 1.6. The variation of lift, drag, and pitching-moment coefficients with angle of attack for the model with controls undeflected is presented in Fig. 5. The lift data show an increase in slope and linearity with decreasing Mach number. The pitching-moment curves also become more linear. The model is stable at trimmed conditions. The stability level increases and the trim angle of attack decreases with decreasing Mach number. At Mach numbers of approximately 3.0 through 1.6, the configuration is trimmed at α=0 deg or slightly negative angles of attack that produce negative lift and *L/D*. Therefore, pitch-control input will be required to trim the vehicle to positive lift in this Mach range. The untrimmed $(L/D)_{max}$ values vary from 1.5 to 1.7 for the Mach range from 4.5 to 1.6.

The lateral stability characteristics are presented in Fig. 6. The HL-20 is directionally stable at angles of attack above 8 deg over the supersonic test range. At Mach numbers from 4.5 to 2.5, directional stability drops to zero or becomes negative at the lower angles of attack. The effective dihedral parameter follows the same trend showing positive effectiveness ($-C_{l_\beta}$) about α=4 or 8 deg. Therefore, the HL-20 with controls undeflected has neutral directional stability and low values of effective dihedral at trim conditions from Mach 2.0 to 3.0. At Mach 1.6, the HL-20 has regained directional stability at low angles of attack.

Pitch-control effectiveness is presented in Fig. 7 using elevons or body flaps alone as pitch control. Data were taken for control deflections up to ±30 deg. Elevons are effective in trimming the model to α=20 deg at Mach 4.5. At Mach 1.6, however, where the HL-20 has a high level of longitudinal stability, the elevons are effective in trimming the model only up to α=4 deg.

Body flaps were about as effective as the elevons. The trim range at Mach 4.5 is from α=2 to 17 deg and about α=−2 to 3 deg at Mach 1.6. Unlike elevons, body flaps are more effective when deflected downward (positive direction). In general then, there is little difference in pitch effectiveness between the elevons or body flaps in the supersonic speed range.

Roll control is accomplished through differentially deflecting the elevons on the outboard fins, Fig. 8a, or the body flaps on the upper aft body, Fig. 8b. Because the longitudinal data suggested a need to trim the configuration to more positive angles of attack (at least at the low-supersonic Mach numbers), only negative control deflections are shown. The effectiveness values are for a case with the left upper elevon or left body flap set at −10 deg, while the right control remained at 0 deg. These deflections represent −5 deg aileron deflection about a −5 deg elevon setting.

The elevons, with their larger transverse moment arm, were much more effective than the body flaps. The effectiveness of both sets of controls is small and decreased with increasing Mach number. The effectiveness of the upper body flaps became zero at Mach 3.0. The simultaneous deflection of elevons and body flaps was not tested.

Differential deflection of the elevons produced as much adverse yawing moment $-\Delta C_n$ as rolling moment. This is because of the rolled-out fin configuration. Differential deflection of the elevons acted as much like a rudder as ailerons. The yawing moment associated with body-flap deflection, on the other hand, is near zero (at Mach numbers where the body flap had any effectiveness). Therefore, if the elevons are used for roll control, a control device, such as a rudder, may be needed to offset the yawing moments produced.

Yaw control is accomplished by pivoting the small center fin about its midchord. Yaw effectiveness data are given in Fig. 9. These data are for a fin deflection of 5 deg. Yaw ΔC_n is essentially constant over the angle-of-attack range at each Mach number. Center-fin effectiveness increased with decreasing Mach number. Unlike differential elevon deflection, the center fin produced almost no crosscoupled moment, that is, no rolling moment. The effectiveness of the center fin as a yaw control, however, is low at these test Mach numbers.

Transonic Speeds

Tests in this speed range were conducted in the Calspan 8-ft Transonic Tunnel. Again, as with flight at supersonic speeds, no high-performance characteristics are necessary. It is desirable, however, to fly at low or moderate angles of attack to reduce possible buffeting and, of course, sufficient control authority is required.

The longitudinal data for Mach numbers from 1.2 to 0.6 are given in Fig. 10. The increase in lift curve slope and increase in

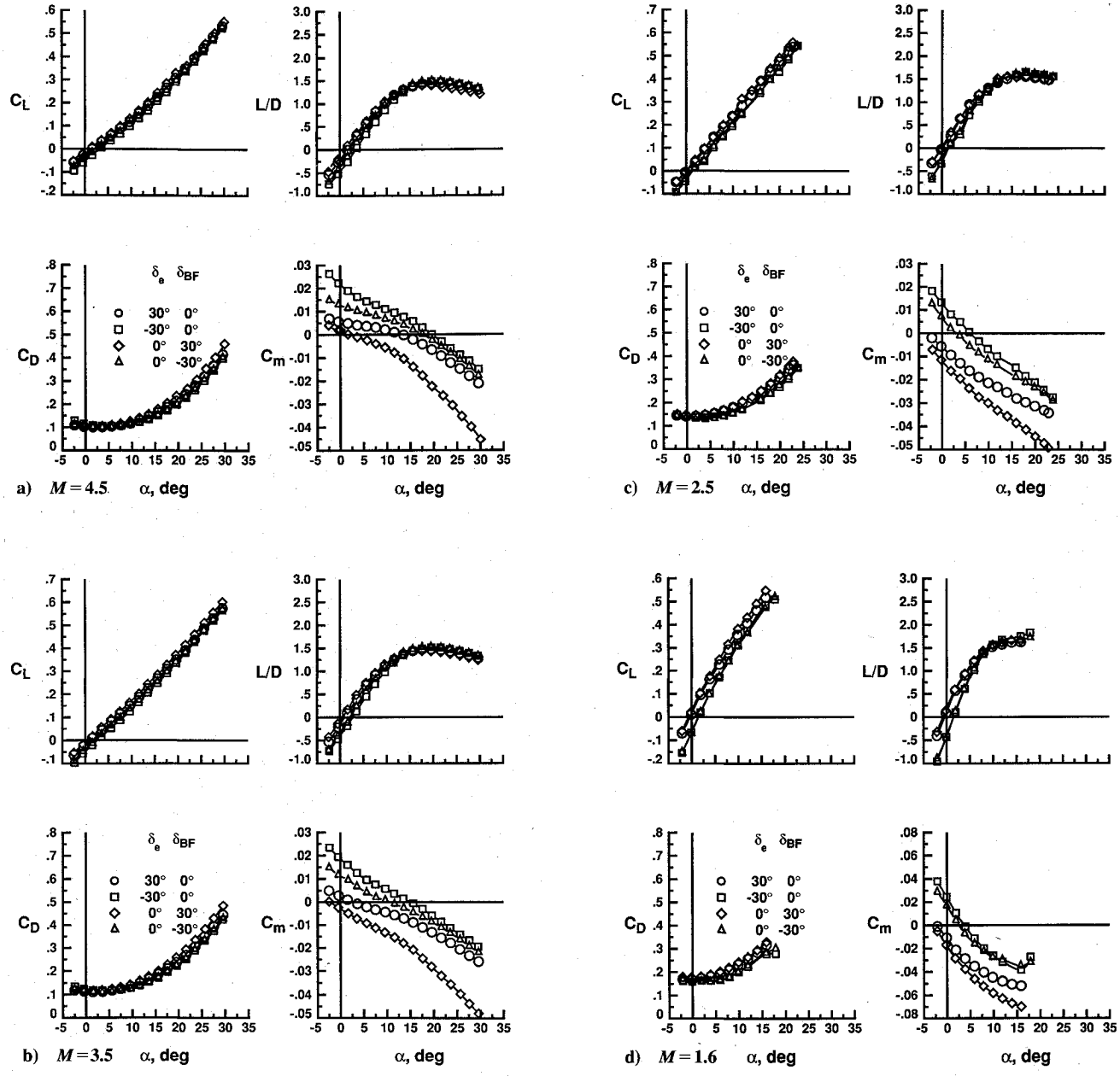

Fig. 7 Pitch-control effects at supersonic speeds.

stability noted in the supersonic tests continue at Mach 1.2. As the speed reaches Mach 1.0, longitudinal stability decreases but the vehicle is very stable (static margin of 5% body length) even at Mach 0.6. The pitching moments exhibit an unstable pitch-up at angles of attack from 15 to 20 deg, depending on Mach number. The model becomes longitudinally unstable at the higher angles at Mach numbers of 0.8 and greater. At all Mach numbers, the destabilizing pitch-up conditions occur at angles of attack above desired flight angles. The HL-20 trim angle increases from 3 deg at Mach 1.2 to about 12 deg at Mach 0.6.

The directional stability characteristics for Mach 1.2 to 0.6 are shown in Fig. 11. The model is directionally stable over the test range at supersonic Mach numbers. From Mach 0.95 to 0.6, there are regions of directional instability at the higher angles of attack. Again, instability occurred at angles above those anticipated in flight (above $\alpha=16$ deg). The model has large values of positive effective dihedral ($-C_{l_\beta}$) over the Mach range.

The transonic longitudinal control effectiveness is presented in Fig. 12. In this speed range, body flaps are not as effective as elevons at the lower angles of attack. At the higher angles of attack, however, flap deflection causes the previously mentioned destabilizing break in pitching moment to occur at lower angles of attack than elevon deflection. Thus, at Mach 0.6 and 0.8, negative body-flap deflection is as effective in trimming the configuration as the elevons. At these lower Mach numbers, a deflection of -10 deg with either elevons or body flaps trims the model to its highest subsonic lift before the onset of longitudinal instability.

The effectiveness of the elevons and body flaps as a roll control is shown in Fig. 13. For these data, the left elevon was deflected -5 deg and right elevon 5 deg. Because the body flaps had a shorter lateral moment arm, they were deflected ± 10 deg. As at supersonic speeds, both sets of controls are effective in producing rolling moments. The elevons with their outboard location are more effective than the body flaps, but only at the lower angles of attack. The effectiveness of the elevons decreases with increasing angle of attack, whereas that of the body flaps remains approximately constant. At the higher angles, the body flaps are as effective as the elevons. Again, the elevons produce about as much adverse yawing moment as rolling moment. The yawing moment associated with body-flap deflection still remained near zero.

Therefore as at supersonic speeds, if elevons are used for roll control, a control device is needed to offset the yawing moments produced.

Yaw-control effectiveness data are given in Fig. 14. The center fin performs at transonic speeds as it did at supersonic speed. The effectiveness value per degree of deflection is essentially constant over the angle-of-attack range and produces almost no crosscoupled moment. The center fin is an effective yaw control device at these transonic speeds.

Subsonic Speeds

The subsonic data presented are from the 7×10-ft High Speed Tunnel (except for Reynolds number effects from the Low-Turbulence Pressure Tunnel). Fig. 15 shows the effect of increasing the Reynolds number from 3.5×10^6 to 22×10^6 (based on body length) on the aerodynamic characteristics of the model. There is little change in lift or pitching moment due to increasing Reynolds num-

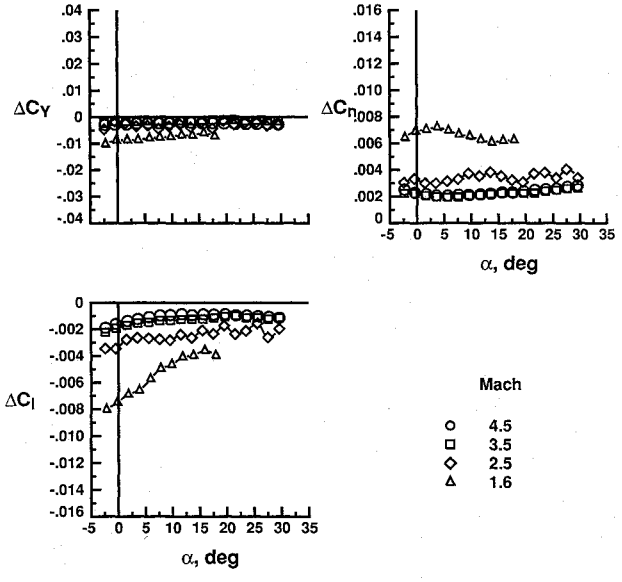

a) Elevon deflection: $\delta_{e,l} = -10$ deg, $\delta_{e,r} = 0$ deg

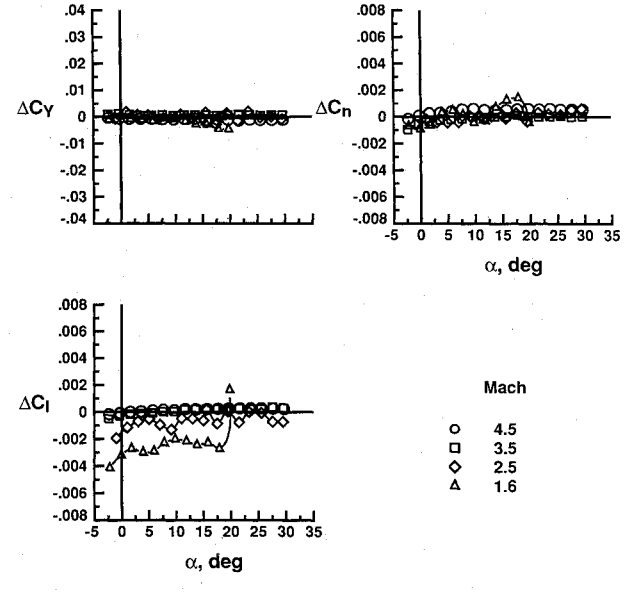

b) Body-flap deflection: $\delta_{BF,l} = -10$ deg, $\delta_{BF,r} = 0$ deg

Fig. 8 Roll-control effects at supersonic speeds.

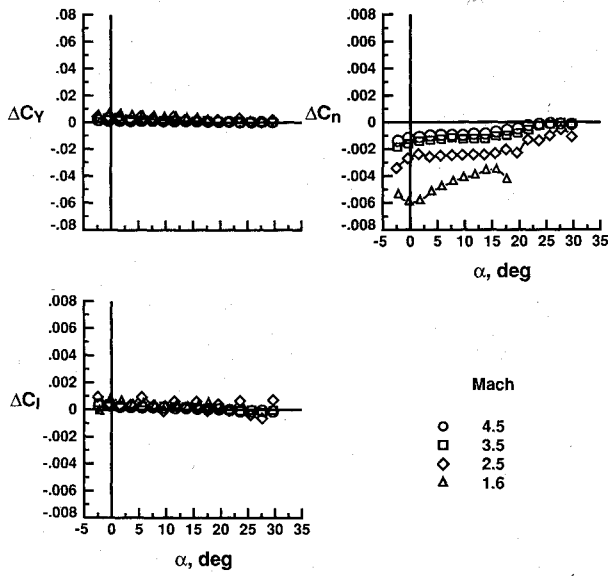

Fig. 9 Center-fin yaw-control effects at supersonic speeds: $\delta_r = 5$ deg.

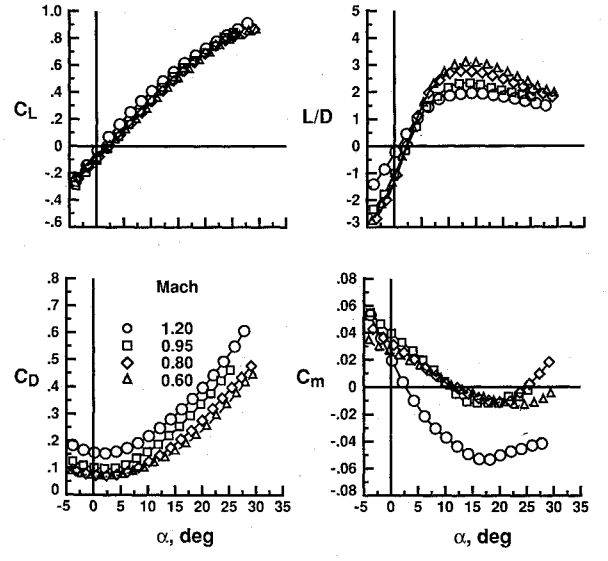

Fig. 10 Longitudinal aerodynamic characteristics at transonic speeds.

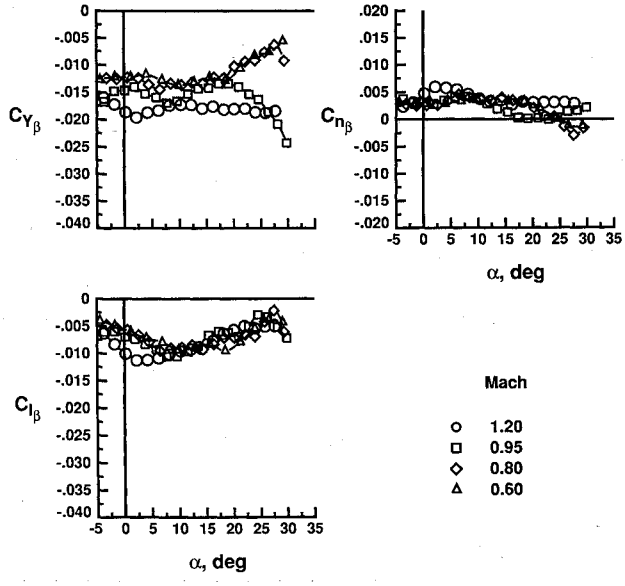

Fig. 11 Lateral aerodynamic characteristics at transonic speeds.

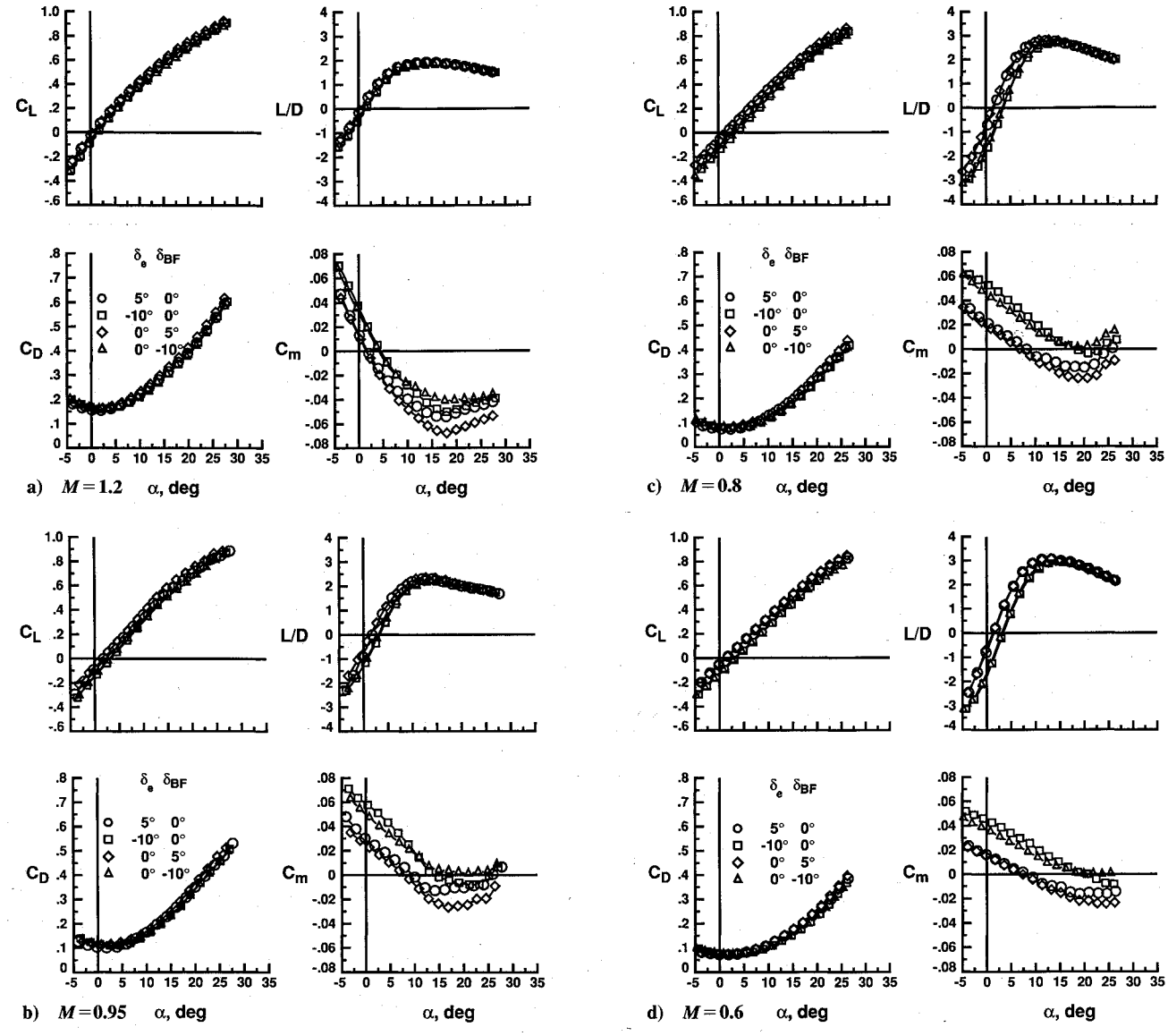

Fig. 12 Pitch-control effects at transonic speeds.

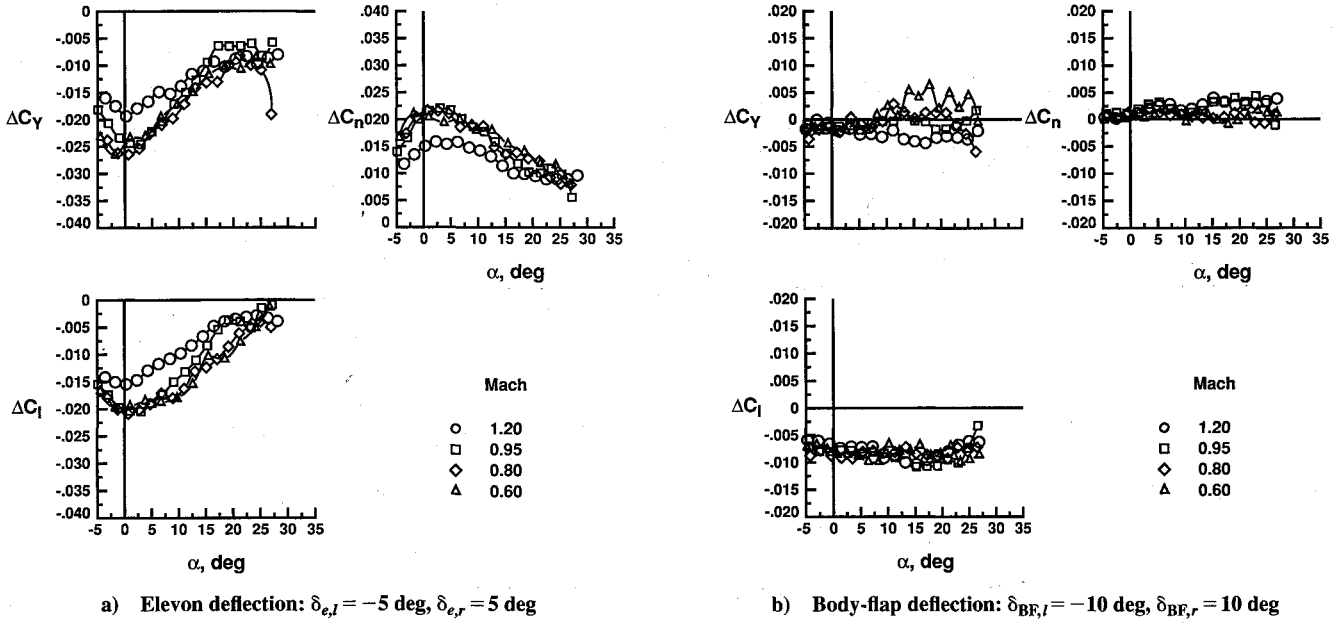

Fig. 13 Roll-control effects at transonic speeds.

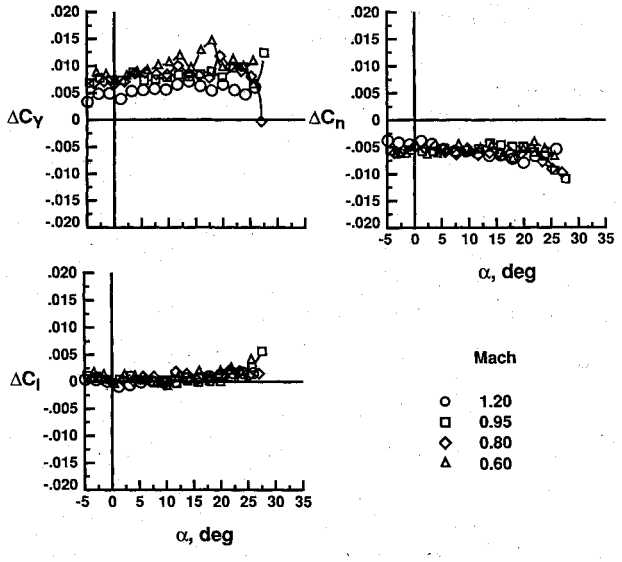

Fig. 14 Center-fin yaw-control effects at transonic speeds: $\delta_r = 5$ deg.

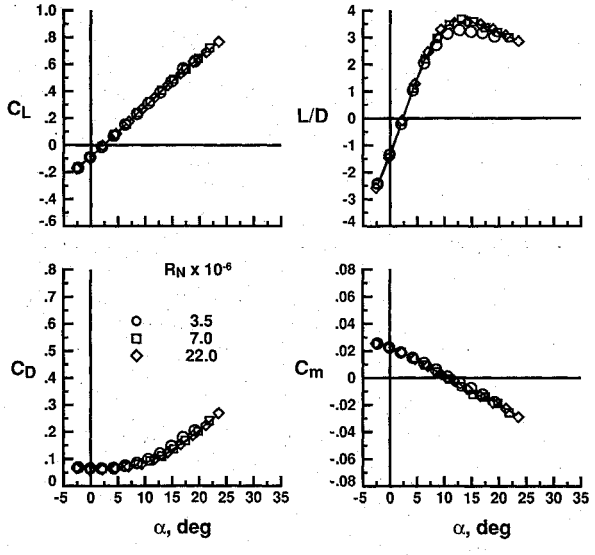

Fig. 15 Reynolds number effects on longitudinal aerodynamic characteristics at subsubsonic speeds: $M = 0.3$.

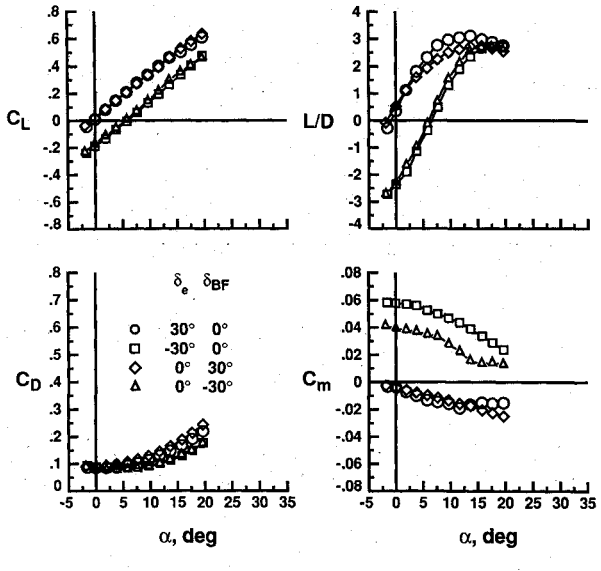

Fig. 16 Pitch-control effects on longitudinal aerodynamic characteristics at subsonic speeds: $R_N = 7 \times 10^6$, $M = 0.3$.

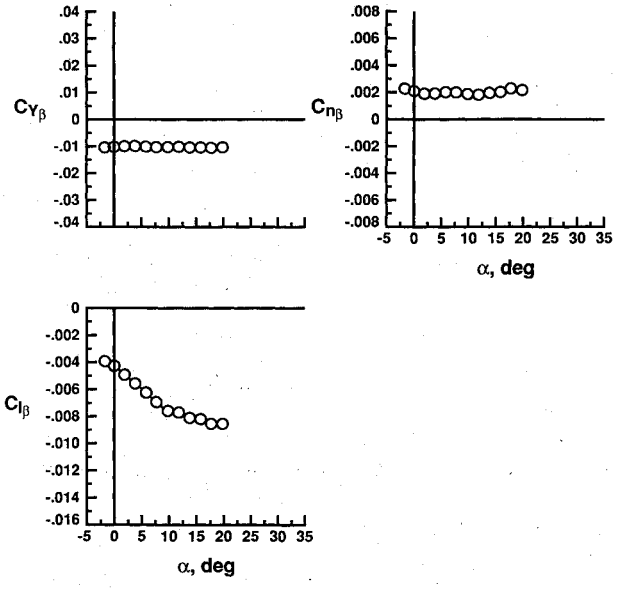

Fig. 17 Lateral aerodynamic characteristics at subsonic speeds: $M = 0.3$.

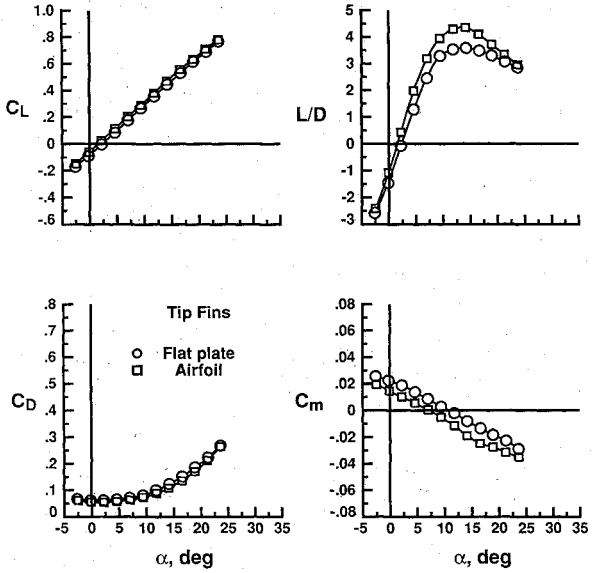

Fig. 18 Effect of tip-fin airfoil on longitudinal aerodynamic characteristics at subsonic speeds: $R_N = 22 \times 10^6$, $M = 0.3$.

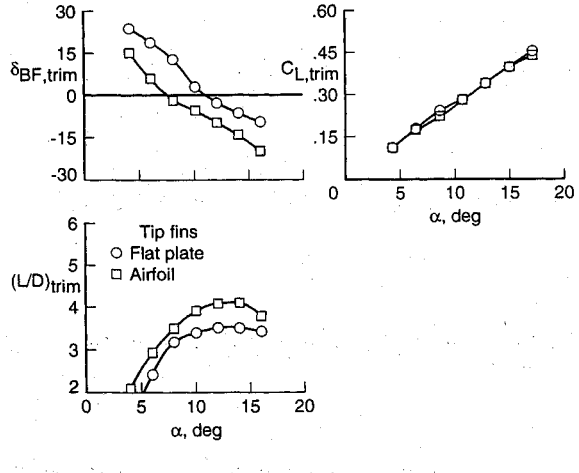

Fig. 19 Longitudinal trim characteristics at subsonic speeds: $M = 0.3$.

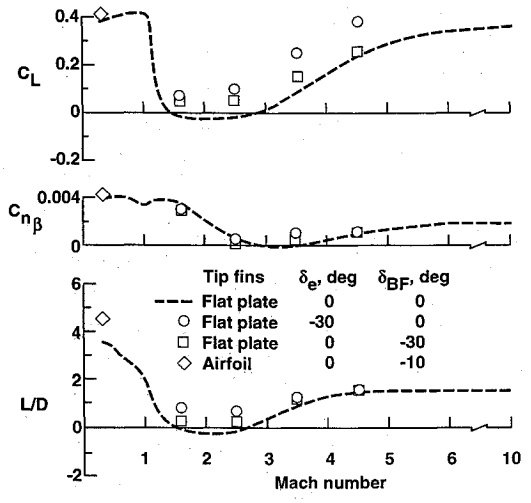

Fig. 20 Summary of trimmed aerodynamic characteristics over Mach range.

ber, but a sufficient change in drag occurs to increase the *L/D* from 3.2 to 3.6. A full-scale-flight Reynolds number based on a 28-ft-long vehicle is approximately 60×10^6 at a landing speed of 200 knots. Note that above a test Reynolds number of 7×10^6, the longitudinal parameters remain relatively constant, suggesting that data taken at the higher Reynolds numbers of the test reflect full-scale vehicle performance. The model is longitudinally stable and trimmed with controls undeflected at about an angle of attack of 11 deg. This trim angle produces an *L/D* of 3.6, which is approximately $(L/D)_{max}$. Longitudinal control with deflections of ±30 deg (Fig. 16) is sufficient with either elevons or body flaps in trimming the model from slightly negative angles of attack to at least $\alpha=20$ deg. The model is also directionally stable (Fig. 17) to angles of attack above $\alpha=20$ deg, which is above projected subsonic flight angles.

The lateral control characteristics of the elevons, body flaps, and rudder at Mach 0.3 are not presented, but are about the same values as those at Mach 0.6 and discussed in the previous section. That is, both elevons and body flaps represent effective roll control (with elevons producing about as much rolling moment as yawing moment) and rudder deflection an effective yaw control.

During the flight simulation investigation in both fixed- and moving-base cockpits, the subsonic control characteristics were found to be satisfactory.[9] Subsonic performance, however, with an $(L/D)_{max}$ of 3.2 or 3.6 was insufficient to meet a Cooper-Harper level 1 handling qualities rating in the pilot-in-the-loop approach and landing simulations. As a result, the tip fins were changed from a flat-plate airfoil shape to a cambered airfoil with a flat undersurface. (See Fig. 2.) The effect of this fin change is shown in Fig. 18. The model lift is increased and drag reduced, resulting in an increase of $(L/D)_{max}$ to 4.3. Because the increase in lift occurred aft of the model *cg*, longitudinal trim is shifted from 11 to 7 deg. The characteristics of the HL-20 with airfoil tip fins trimmed with body-flap deflection, Fig. 19, indicate an $(L/D)_{max}$ of approximately 4.2. This represents a significant improvement of 0.6 in. $(L/D)_{trim}$ over that of the model with flat-plate fins. When the improved aerodynamic performance values of the HL-20 with modified fins were installed in the simulator, the resulting "flights" were improved enough to upgrade handling qualities to level 1 (Ref. 9).

Summary Aerodynamics

The aerodynamics of the HL-20 are summarized as the variation of the trimmed values of lift coefficient, directional stability parameter C_{n_β}, and *L/D* ratio plotted against Mach number in Fig. 20. Data are shown for the HL-20 with controls undeflected and with elevons and body flaps deflected −30 deg over the supersonic speed range. With controls neutral, the HL-20 trims at hypersonic and subsonic conditions with an $(L/D)_{max}$ of 1.4 and 3.6, respectively. (With airfoil fins, subsonic $(L/D)_{max}=4.2$.) Except for the speed range from about Mach 3.5 to 1.5, pitch-control input is unnecessary for stable trim with positive lift. The model has positive directional stability at all speeds except around Mach 2.0. With −30-deg pitch control with either elevons or body flaps, the vehicle is trimmed with positive lift and *L/D* over the Mach range, but in the Mach range around 2.0, the values remain low.

Concluding Remarks

The aerodynamic characteristics of the HL-20 lifting-body configuration have been investigated in wind-tunnel tests from hypersonic to subsonic speeds. The data show that the HL-20 is longitudinally and laterally stable over the complete test Mach range. At hypersonic speeds, the trimmed *L/D* ratio is 1.4. This value gives the vehicle a crossrange capability slightly greater than that of the Space Shuttle. At subsonic speeds, the HL-20 has a trimmed *L/D* ratio of about 3.6. Replacing the flat-plate outboard fins with fins having an airfoil shape increased the maximum trimmed subsonic *L/D* to 4.2.

References

[1]Stone, H. W., and Piland, W. M., "21st Century Space Transportation System Design Approach: HL-20 Personnel Launch System," *Journal of Spacecraft and Rockets*, Vol. 30, No. 5, 1993, pp. 521–528.

[2]Ware, G. M., Spencer, B., Jr., and Micol, J. R., "Aerodynamic Characteristics of Proposed Assured Crew Return Capability (ACRC) Configurations," AIAA Paper 89-2172, July 1989.

[3]Ware, G. M., "Transonic Aerodynamic Characteristics of a Proposed Assured Crew Return Capability (ACRC) Lifting-Body Configuration," NASA TM 4117, June 1989.

[4]Ware, G. M., "Supersonic Aerodynamic Characteristics of a Proposed Assured Crew Return Capability (ACRC) Lifting-Body Configuration," NASA TM 4136, Nov. 1989.

[5]Cruz, C. I., Ware, G. M., Grafton, S. B., Woods, W. C., and Young, J. C., "Aerodynamic Characteristics of a Proposed Personnel Launch System (PLS) Lifting-Body Configuration at Mach Numbers from 0.05 to 20.3," NASA TM 101641, Nov. 1989.

[6]Micol, J. R., "Experimental and Predicted Aerodynamic Characteristics of a Proposed Assured Crew Return Vehicle (ACRV) Lifting Body Configuration at Mach 6 and 10," AIAA Paper 90-1403, June 1990.

[7]Ware, G. M., Spencer, B., Jr., and Micol, J. R., "Aerodynamic Characteristics of the HL-20 and HL-20A Lifting-Body Configurations," AIAA Paper 91-3215, Sept. 1991.

[8]Powell, R. W., "Six-Degree-of-Freedom Guidance and Control Analysis of the HL-20," *Journal of Spacecraft and Rockets*, Vol. 30, No. 5, 1993, pp. 537–542.

[9]Jackson, E. B., Rivers, R. A., and Bailey, M. L., "Effect of Lift to Drag Ratio in Pilot Rating of the HL-20 Landing Task," *Journal of Spacecraft and Rockets*, Vol. 30, No. 5, 1993, pp. 543–548.

[10]Naftel, J. C., and Talay, T. A., "Ascent Abort Capability for the HL-20," *Journal of Spacecraft and Rockets*, Vol. 30, No. 5, 1993, pp. 628–634.

[11]Penaranda, F. E., and Freda, M. S., (eds.), "Aeronautical Facilities Catalogue. Volume I - Wind Tunnels," NASA RP-1132, 1985.